Neutron Star Properties and Femtoscopic Constraints

Isaac Vidaña, INFN Catania



NUSDAF 2025: First Collaboration Meeting on Nuclear Structure, Dynamics & Astrophysics Octobre 22<sup>th</sup>-24<sup>th</sup> 2025 INFN, Catania



## A bit of motivation for this work

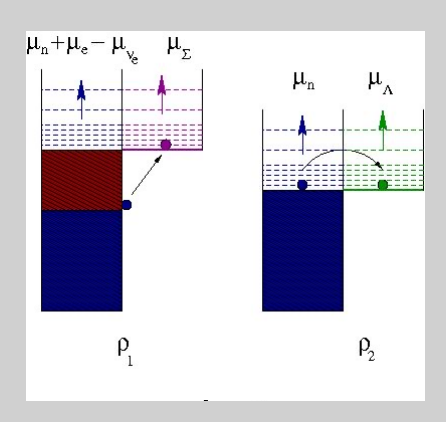
#### • In general:

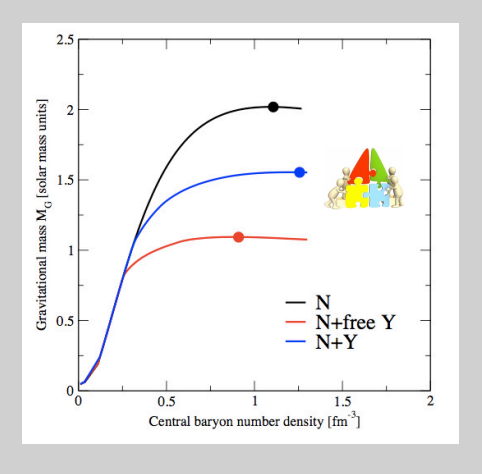
The presence of hyperons in finite (hypernuclei) & infinite (neutron stars) nuclear systems allow the study of baryon-baryon interactions from an enlarge perspective extending our present knowledge of conventional nuclear physics to the SU(3)-flavor sector

#### In particular:

The determination of the hypernuclear EoS is fundamental to understand many properties of neutron stars (masses, cooling, gravitational instabilities, ...) which can be affected by the presence of hyperons

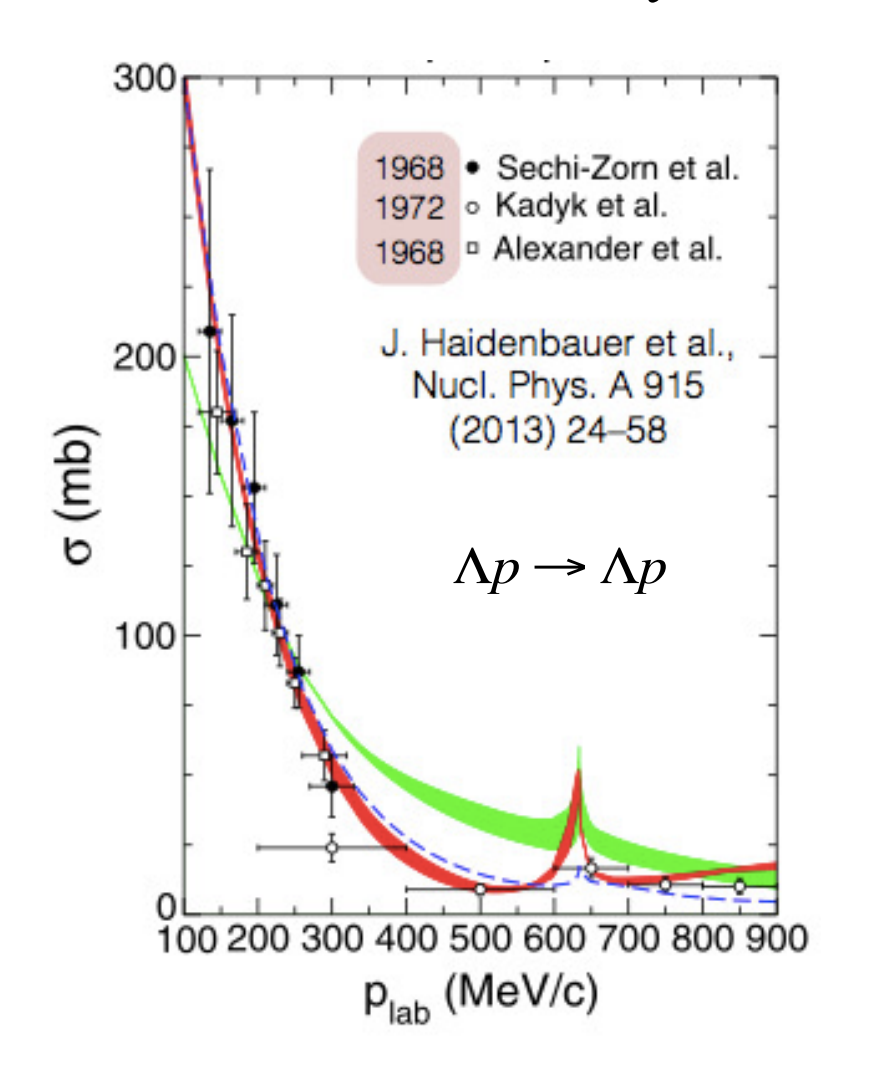
For intance, the hyperon puzzle, the problem of the strong softening of the EoS induced by the presence of hyperons which, although being energetically favorable, leads to values of  $M_{max}$  incompatible with the recent observations of  $2M_{\odot}$  millisecond pulsars, is still an open issue





The main ingredients to understand the role of hyperons in NSs are the YN &YY interactions. But how much do we know to constrain them?

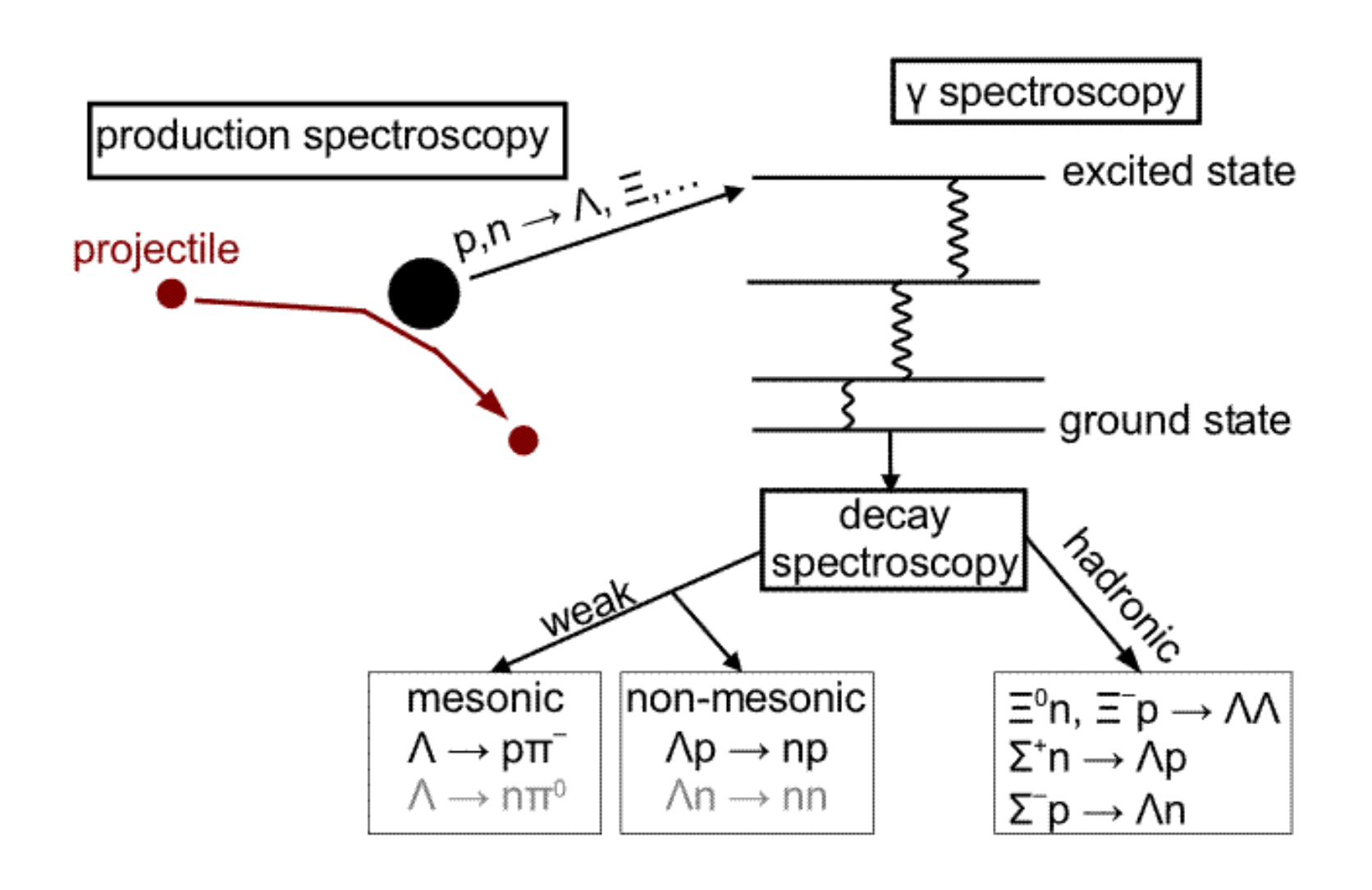
## Unfortunately, much less than in the pure nucleonic sector



- Very few YN scattering data due to short lifetime of hyperons & low intensity beam fluxes
  - $\sim$  35 data points, all from the 1960s
  - 10 new data points, from KEK-PS E251 collaboration (2000)
  - No YY scattering data exists

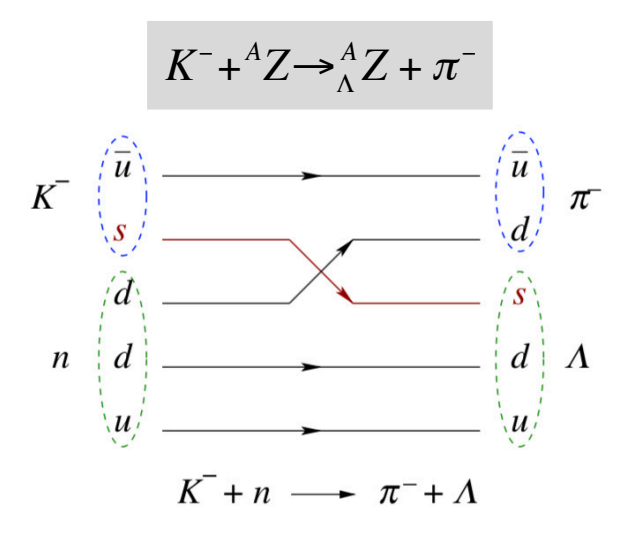
(cf. > 4000 NN data for  $E_{lab} < 350$  MeV)

Alternative & complementary information can be obtained from the study of hypernuclei (bound systems of nucleons & hyperons) with the goal of relating hypernuclear observables with the underlying bare YN & YY interactions



## Production of single-Λ hypernuclei

### **♦ Strangeness exchange (BNL, KEK, JPARC)**

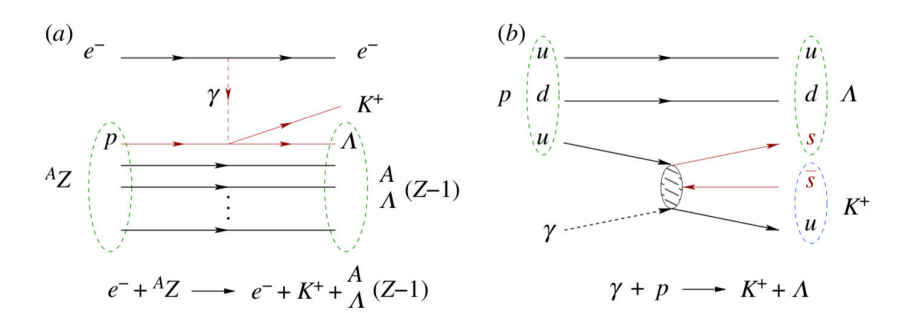


(replace an u or d quark by an s one)



## **♦ Electroproduction (JLAB, MAMI-C)**

$$e^{-} + {}^{A}Z \rightarrow e^{-}' + K^{+} + {}^{A}_{\Lambda}(Z - 1)$$



### **♦** Associate production (BNL, KEK, GSI)

→ Hypernuclei production in relativistic heavy ion collisions (HypHII collaboration FAIR/GSI)

First experiment with  $^6\text{Li}$  beam on  $^{12}\text{C}$  target at 2GeV.  $\Lambda$ ,  $^3_{\Lambda}\text{H}$  &  $^4_{\Lambda}\text{H}$  observed.

## Production of double-Λ hypernuclei

Best systems to investigate the properties of S = -2 baryon—baryon interaction

Contrary to single- $\Lambda$  hypernuclei they are produced in a two-step process

- ➤ Ξ<sup>-</sup> production in process like
  - ✓ (K<sup>-</sup>,K<sup>+</sup>) reaction (BNL, KEK)

$$K^- + p \rightarrow \Xi^- + K^+$$

✓ Proton-antiproton reaction (GSI/FAIR)

$$p + \overline{p} \rightarrow \Xi^- + \overline{\Xi}^+$$

 $\triangleright$   $\Xi^-$  captured in an atomic orbit interacts with the nuclear core producing two  $\Lambda$ 's

$$\Xi^- + p \rightarrow \Lambda + \Lambda + 28.5 \, MeV$$

Binding energy  $\Delta B_{\Lambda\Lambda}$  of two  $\Lambda s$  in double- $\Lambda$  hypernuclei

$$\Delta B_{\Lambda\Lambda}({}_{\Lambda\Lambda}^{A}Z) = B_{\Lambda\Lambda}({}_{\Lambda\Lambda}^{A}Z) - 2B_{\Lambda}({}_{\Lambda}^{A-1}Z) = B_{\Lambda}({}_{\Lambda\Lambda}^{A}Z) - B_{\Lambda}({}_{\Lambda}^{A-1}Z)$$

Earlier emulsion experiments reported the formation of  $^{6}_{\Lambda\Lambda}$ He,  $^{10}_{\Lambda\Lambda}$ Be &  $^{13}_{\Lambda\Lambda}$ B but the identification of the last two was ambiguous. The value of the Nagara event recently revised  $\Delta B_{\Lambda\Lambda} = 0.67 \pm 0.17$  MeV due to a change of the  $\Xi^{-}$ mass

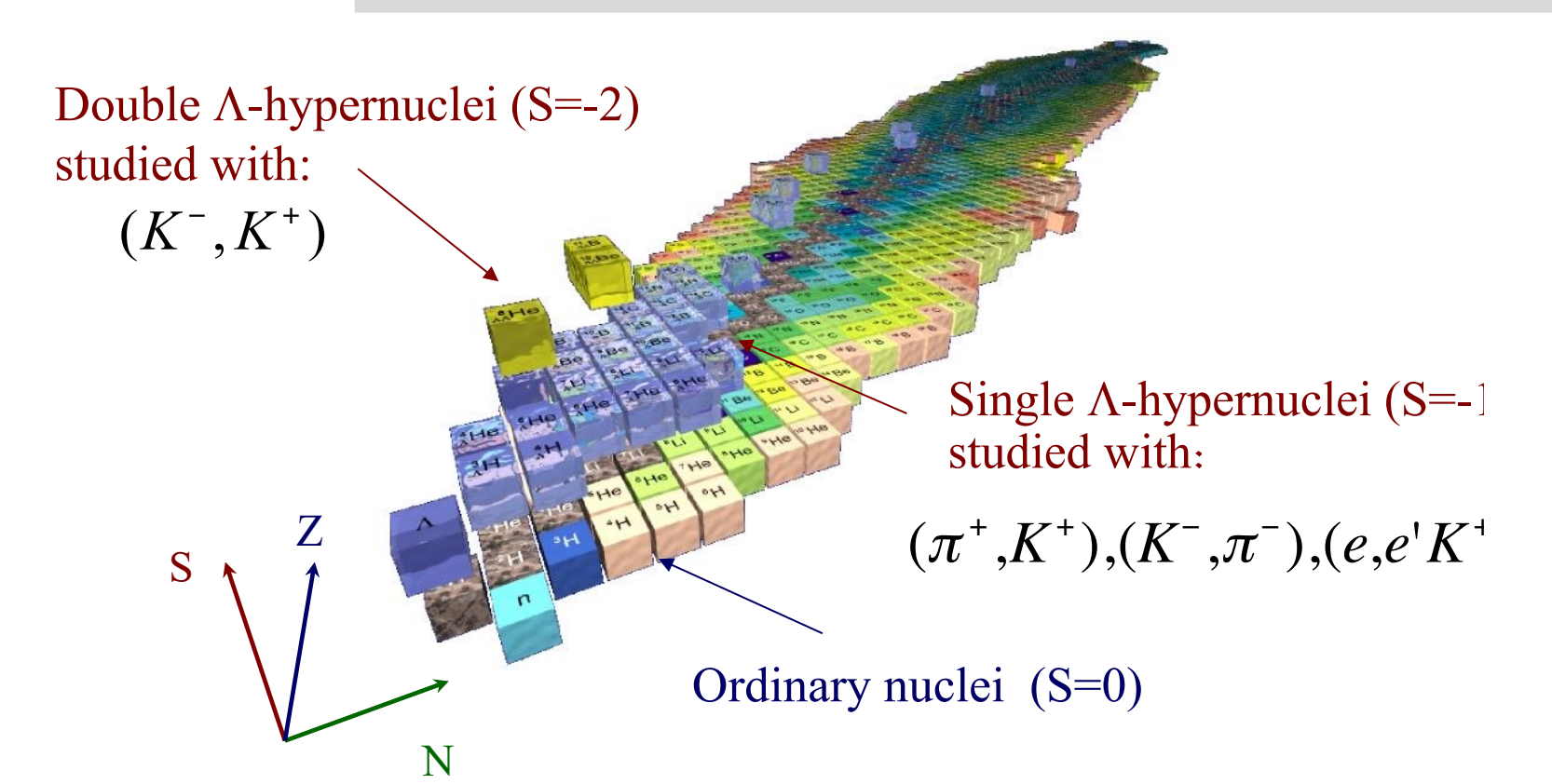
		$B_{\Lambda\Lambda}$ (MeV)	$\Delta B_{\Lambda\Lambda}$ (MeV)	Nagara
	<sub>лл</sub> <sup>6</sup> Не	$10.9 \pm 0.5$	$4.7 \pm 0.6$	Prowse (1966) event
	<sub>лл</sub> <sup>6</sup> Не	$7.25 \pm 0.19^{+0.18}_{-0.11}$	1.01±0.20 <sup>+0.18</sup> <sub>-0.11</sub>	KEK-E373 (2001)
b.	10 <b>Be</b>	$17.7 \pm 0.4$	4.3 ± 0.4	Danysz (1963) same
	10 <b>Be</b>	$8.5 \pm 0.7$	$-4.9 \pm 0.7$	KEK-E176 (1991) event
	13 <b>B</b>	$27.6 \pm 0.7$	$4.8 \pm 0.7$	KEK-E176 (1991)
	10 <b>Be</b>	12.33 <sup>+0.35</sup> <sub>-0.21</sub>		KEK-E373 (2001, unpublished)

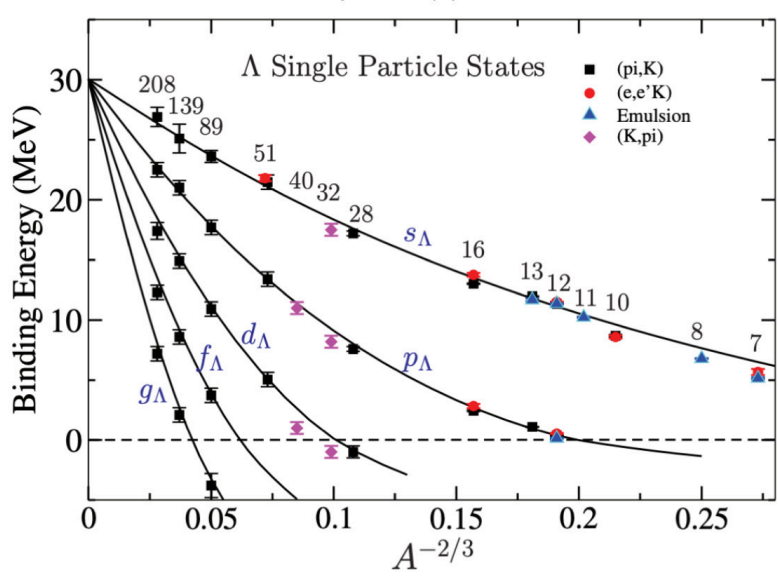
## Production of single- $\Sigma$ and single- $\Xi$ hypernuclei

- ✓ Production of single-Σ hypernuclei mechanisms similar to the ones considered for Λ hypernuclei like, e.g., strangeness exchange  $(K^-, \pi^\pm)$ . However, their existence has not been experimentally confirmed yet without ambiguity, suggesting that the Σ nucleon interaction is most probably repulsive.
- ✓ Single- $\Xi$  hypernuclei can be produced by means of (K<sup>-</sup>, K<sup>+</sup>) & proton-antiproton reactions
  - A first analysis [1] of  ${}^{12}C(K^-, K^+)^{12}_{\Xi}$ Be reaction indicated an attractive  $\Xi$ -nucleus interaction of the order of about -14 MeV, but an independent analysis [2] of the  $(K^-, K^+)\Xi$  production spectrum on  ${}^{12}C$  found instead an almost zero  $\Xi$ -nucleus potential
  - A deeply bound state of the  $\Xi^- {}^{14}N$  system with a binding energy of 4.38  $\pm$  0.25 MeV has been observed [3]. Future  $\Xi$ -hypernuclei production experiments are being planned at JPARC
    - [1] Khaustov et al. PRC 61, 054603 (2000)
    - [2] Kohno et al. PTP 123, 157 (2010); NPA 835, 358 (2010)
    - [3] Nakazawa et al. PTEP 033D02 (2015)

## Summary of our present knowledge & ignorance from hypernuclei

- 41 single  $\Lambda$ -hypernuclei  $\longrightarrow \Lambda N$  attractive ( $U_{\Lambda}(\rho_0) \sim -30 \text{ MeV}$ )
- 3 double- $\Lambda$  hypernuclei  $\longrightarrow$  weak  $\Lambda\Lambda$  attraction ( $\Delta B_{\Lambda\Lambda} \sim 0.67$  MeV)
- Very few  $\Xi$ -hypernuclei  $\longrightarrow \Xi N$  attractive ( $U_{\Xi}(\rho_0) \sim -14 \text{ MeV}$ )
- Ambiguous evidence of Σ-hypernuclei  $\longrightarrow$  ΣN repulsive ( $U_{\Sigma}(\rho_0) > +15$  MeV)?



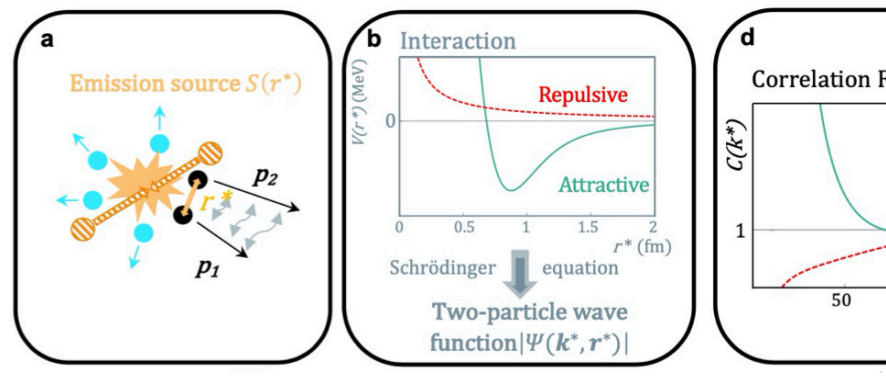


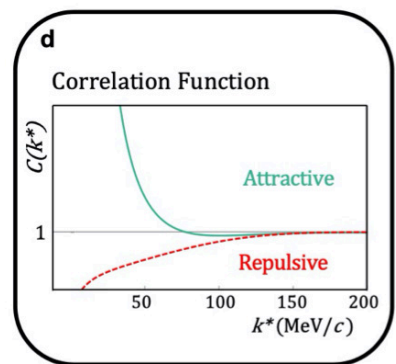
Gal et al. Rev. Mod. Phys. 83, 035004 (2016)

## Constraining hyperon interactions from Femtoscopy

Information on the YN interactions, additional to that from scattering & hypernuclei, together with constraints on the YY ones & three-body forces has begun to be recently available thanks the to **Femtoscopy Technique** by measuring the **correlations** (in momentum space) of YN pairs, YY pairs & YNN triads in *p-p* and *p-Pb* collisions at LHC by the ALICE Collaboration

$$C(k^*) = \frac{N_{SE}(k^*)}{N_{ME}(k^*)} \approx 1 + \int d^3r S(r) \left( |\Psi(k^*,r)|^2 - j_0^2(k^*r) \right)$$
Measurement
(pairs in same event)/(pairs from different events)
Measurement
Koonin-Pratt equation





- S(r): emission source describes the probability of emitting the particle pair at a relative distance r.
- $\Psi(k^*, r)$ : two-particle scattering wave function
  - ✓ Attraction  $\Rightarrow$  enhancement of  $\Psi(k^*, r) \Rightarrow C(k^*) > 1$
  - ✓ Repulsion  $\Rightarrow$  reduction of  $\Psi(k^*, r) \Rightarrow C(k^*) < 1$

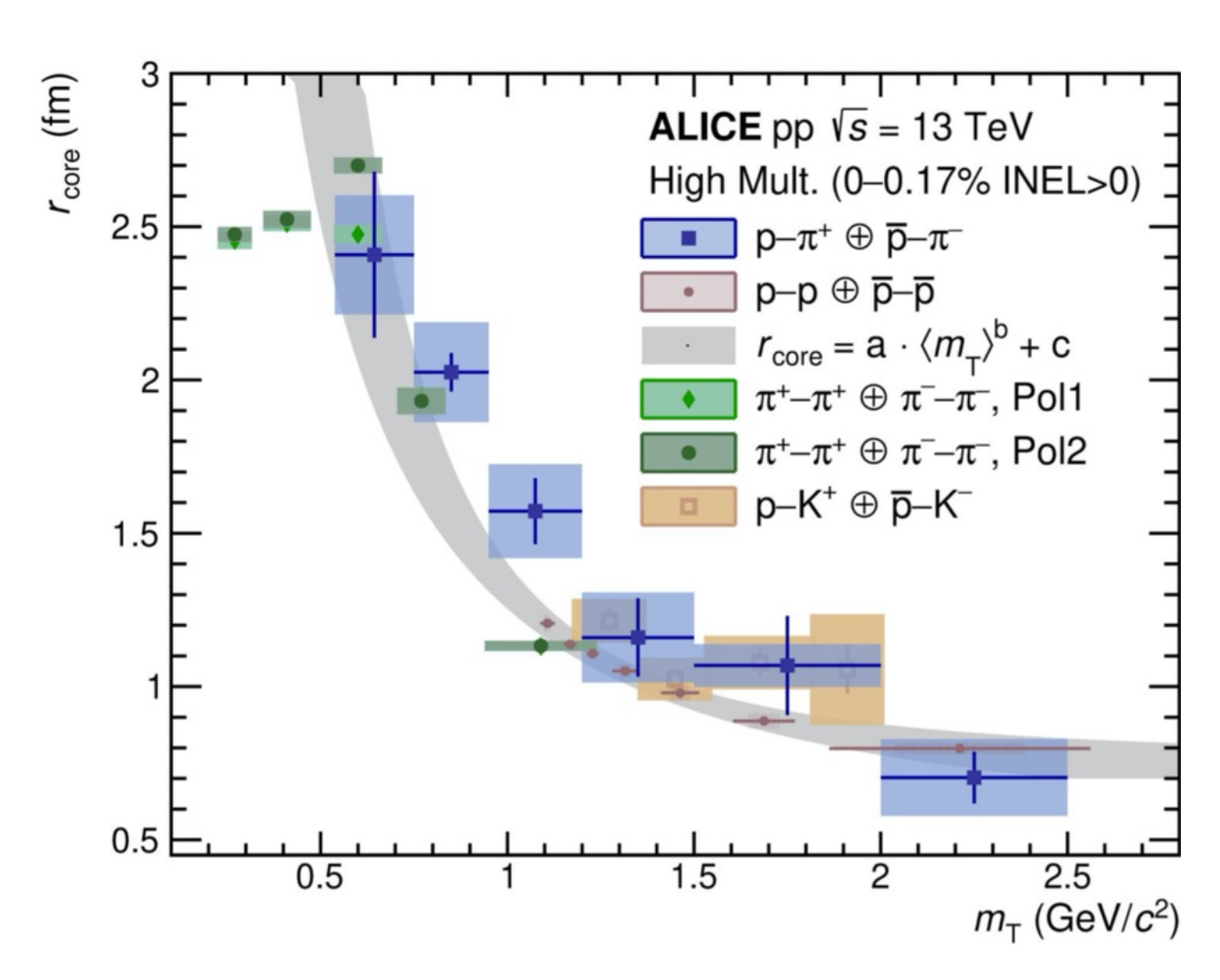
### A Comment on the Emission Source

From the analysis of the two-particle correlation functions of several particle pairs:

- $p \pi^{\pm}$   $\pi^{\pm} \pi^{\pm}$
- $p K^+$

The ALICE collaboration, using known final state interactions (Lednický–Lyuboshits model), found that the extrated source size  $(r_{core})$  as a function of the pair transverse mass  $(m_T)$  supports the idea of a "common emission source" for hadron paies in pp collisions

$$S(r) = \frac{1}{(4\pi r_{core}^2)^{3/2}} exp\left(-\frac{r^2}{4r_{core}^2}\right) + resonace tail$$



ALICE, PLB 811, 135849 (2020); ALICE, EPJ A 61, 194 (2025)

### This talk in few words

- Construction within the BHF approach the hypernuclear matter EoS & study the properties of NSs using a chiral YN interaction from the Jülich-Bonn group tuned to femtoscopic  $p\Lambda$  data of the ALICE Collaboration &  $\Lambda\Lambda$  and  $\Xi N$  interactions determined from LQCD calculations of the HAL QCD Collaboration that reproduce the femtoscopic  $\Lambda\Lambda$  and  $p\Xi^-$  data
- Special attention is put on the uncertainties of the baryon interactions & how they are effectively propagated to the composition, EoS, MR relation & tidal deformability of NSs

#### In collaboration with:

- V. Mantovani-Sarti
- J. Haidenbauer
- D. Mihaylov
- L. Fabbietti

#### For details see:



Eur. Phys. J. A (2025) 61:59

♦ Nucleon-Nucleon interaction: Argonne V18 (AV18)

$$\widehat{V}_{ij}(r_{ij}) = \sum_{p=1}^{18} V_{ij}(r_{ij}) \widehat{O}_{ij}^{p} \quad \text{with} \quad \widehat{O}_{ij}^{p=1,\cdots,14} = \left[1, (\vec{\sigma}_{i} \cdot \vec{\sigma}_{j}), S_{ij}, \vec{L} \cdot \vec{S}, L^{2}, L^{2}(\vec{\sigma}_{i} \cdot \vec{\sigma}_{j}), (\vec{L} \cdot \vec{S})^{2}\right] \otimes \left[1, (\vec{\tau}_{i} \cdot \vec{\tau}_{j})\right] \\ \widehat{O}_{ij}^{p=15,\cdots,18} = \left[T_{ij}, (\vec{\sigma}_{i} \cdot \vec{\sigma}_{j})T_{ij}, S_{ij}T_{ij}, T_{ij}\left(\tau_{z_{i}} + \tau_{z_{j}}\right)\right] : \text{charge symmetry breaking}$$

The AV18 NN potential is supplemented with a phenomenological three-nucleon force to explore the uncertainty on the NSs properties associated to the softness/stiffness of the pure nucleonic part of the EoS

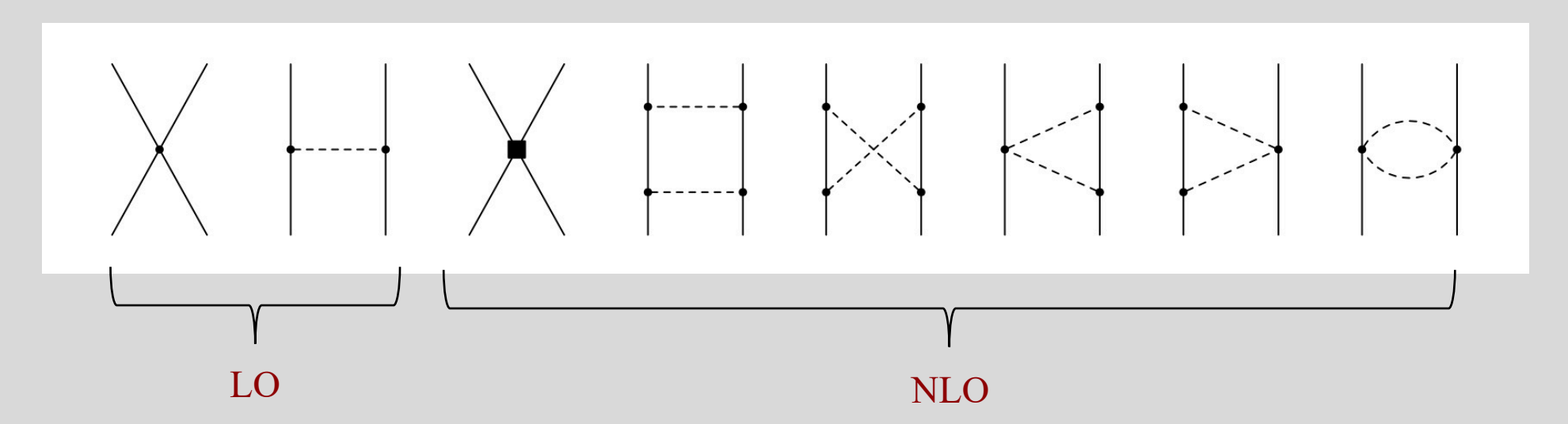
$$\varepsilon_{3NF} = \left(a(\rho_n + \rho_p)^2 + b(\rho_n + \rho_p)^3\right)(1 + \beta^2), \qquad \beta = \frac{\rho_n - \rho_p}{\rho_n - \rho_p}$$

a (MeV fm <sup>3</sup> )	b (MeV fm <sup>6</sup> )	$E_0$ (MeV)	$K_0$ (MeV)
-15.22	21.70	-16	160
-53.42	260.42	-16	270

The coefficients a & b are fitted to reproduce simultaneously the binding energy of SNM at  $\rho_0$ =0.16 fm<sup>-3</sup> and  $K_0$  for which two extreme values compatible with experimental data have been considered corresponding to a soft & a stiff nucleonic EoS

→ Hyperon-Nucleon interaction: chiral NLO19 potential from the Jülich group

Derived within SU(3)  $\chi$ EFT. It incorporates terms up to NLO that include contributions from one- and two-pseudoscalar-meson exchange diagrams involving the Goldstone bosons  $\pi$ , K,  $\eta$  and four-body contact terms with & without two derivatives enconding the short distance dynamics



• LECs associated with the contact terms need to be constrained by experimental data. Established so far by a global fit of  $36 \text{ Ap \& } \Sigma N$  low energy scattering data points. SU(3) flavor symmetry allows to reduce the LECs



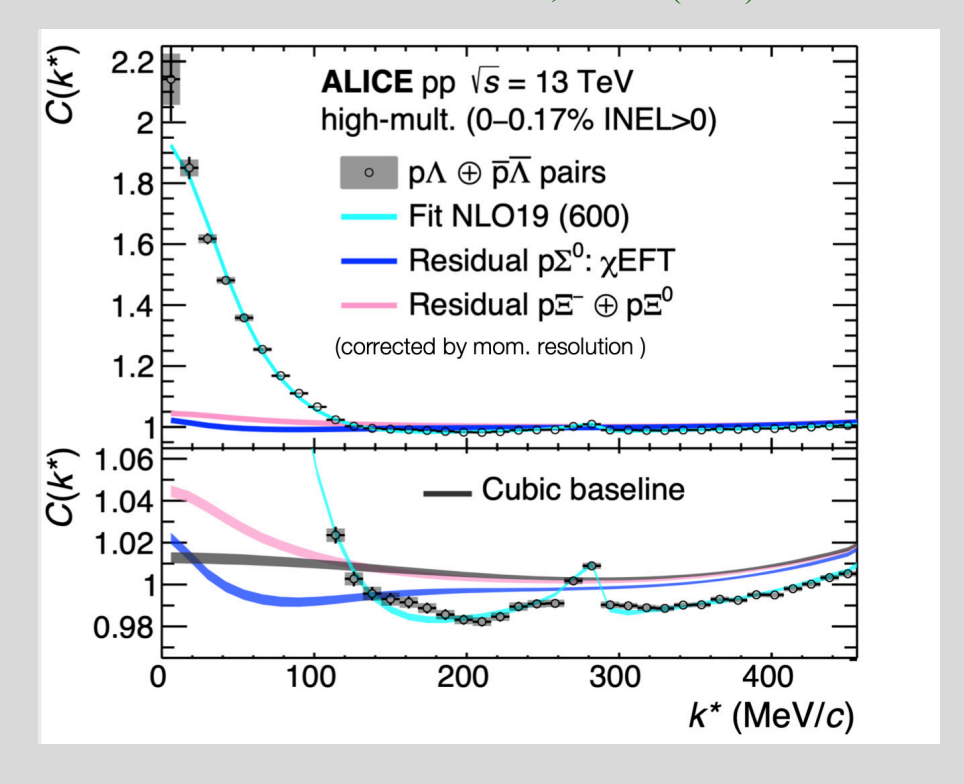
→ Hyperon-Nucleon interaction: chiral NLO19 potential from the Jülich group

• Here we are interested in variants (see Mihaylov et al., PLB 850, 138550 (2024)) of this potential resulting from the combined analysis of scattering data & the \$\Lambda p\$ correlation function measured recently by the ALICE Collaboration

 $\Lambda p$  correlation function data  $\rightarrow$  weaker  $\Lambda N$  interaction than that predicted by the original NLO19 potential. To generate it, SU(3) symmetry breaking is used to fine tune the LECs while keeping the description of the cross sections of other YN reactions unchanged compared with the original NLO19 potential

		$f_0$	$d_0$	$f_1$	$d_1$
NLO19(600)		2.91	2.78	1.41	2.52
variants I	$n_{\sigma} = -1$	2.50	2.95	1.32	2.63
	$n_{\sigma}=0$	2.50	2.95	1.46	2.47
	$n_{\sigma}=1$	2.50	2.95	1.55	2.37
variants II	(500)	2.91	3.10	1.41	2.74
	(550)	2.91	2.93	1.41	2.66
	(650)	2.91	2.65	1.41	2.59

ALICE Col. PLB 833, 137272 (2022)



### ♦ AA & EN interaction: LQCD calculation from the HAL-QCD Collaboration

 $\Lambda\Lambda$ ,  $\Xi N \& \Lambda\Lambda \leftrightarrow \Xi N$  were derived on the basis of (2+1)-flavor LQCD simulations close to the physical point and parametrized as combinations of Gaussians and Yukawa functions

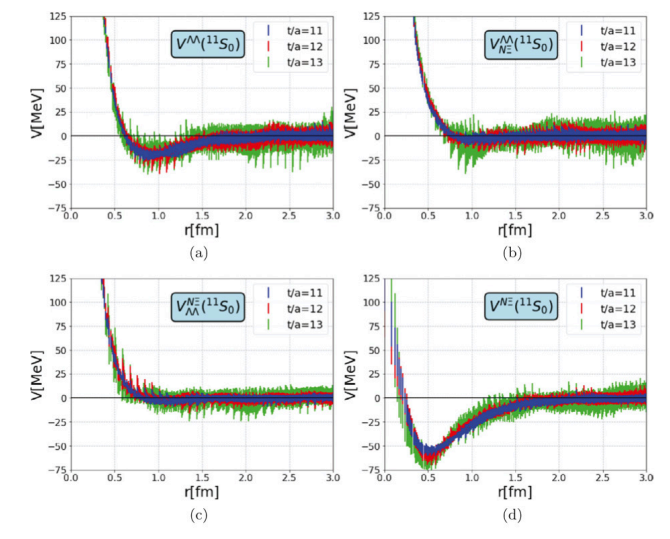
$$V_{C}^{\Lambda\Lambda}(r) = \sum_{i=1}^{2} \alpha_{i}^{\Lambda\Lambda} e^{-\frac{r^{2}}{\beta_{i}^{\Lambda\Lambda^{2}}}} + \lambda_{2}^{\Lambda\Lambda} [\mathcal{Y}(\rho_{2}^{\Lambda\Lambda}, m_{\pi}, r)]^{2} \quad V_{C}^{\Lambda\Lambda-\Xi N}(r) = \sum_{i=1}^{2} \alpha_{i} e^{-\frac{r^{2}}{\beta_{i}^{2}}} + \lambda_{1} [\mathcal{Y}(\rho_{1}, m_{K}, r)]^{2}$$

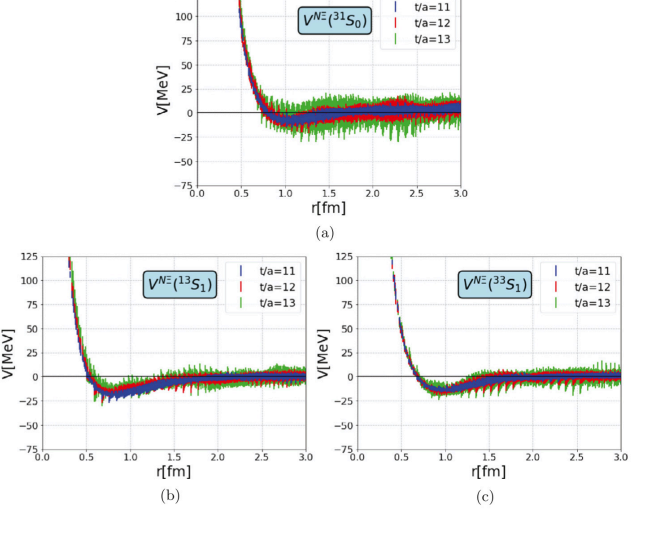
$$V_{C}^{\Xi\Xi}(r) = \sum_{i=1}^{3} \alpha_{i}^{C} e^{-\frac{r^{2}}{\beta_{i}^{2}}} + \lambda_{2}^{C} [\mathcal{Y}(\rho_{2}, m_{\pi}, r)]^{2} + \lambda_{1}^{C} [\mathcal{Y}(\rho_{1}, m_{\pi}, r)]^{2}$$

$$C = {}^{11}S_0, {}^{31}S_0, {}^{13}S_1, {}^{33}S_1, {}^{(2l+1,2S+1}L_l)$$

$$y(\rho, m, r) \equiv \left(1 - e^{-\frac{r^2}{\rho^2}}\right) \frac{e^{-mr}}{r}$$

- AA attractive at low energies but not enough to generate a bound/resonant state
- EN relative strong attraction in (S=0,I=0), weakly repulsive in (S=0,I=1) & weakly attractive in (S=1,I=0) & (S=1,I=1)
- EN used by the ALICE Collaboration in the analysis of  $\Xi^-p$  correlation function. Good agreement between the CF predicted by this potential & measurement







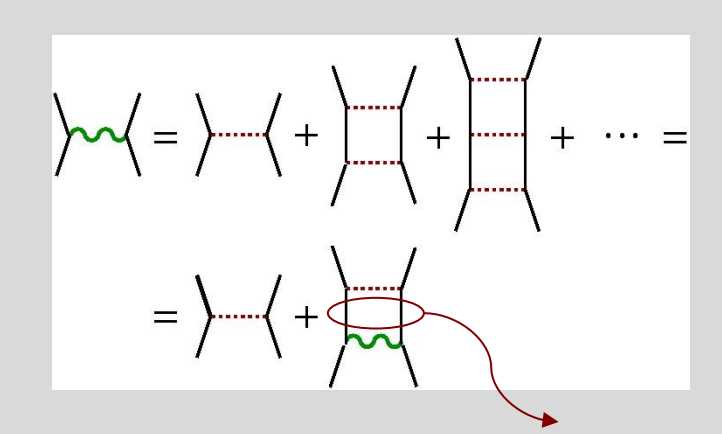
## The BHF approach of hyperonic matter in a nutshell



### **♦** Bethe-Goldstone Coupled Channel Equation

$$G(\omega)_{B_{1}B_{2};B_{3}B_{4}} = V_{B_{1}B_{2};B_{3}B_{4}} + \frac{1}{\Omega} \sum_{B_{i}B_{j}} V_{B_{1}B_{2};B_{i}B_{j}} \frac{Q_{B_{i}B_{j}}}{\omega - E_{B_{i}} - E_{B_{j}} + i\eta} G(\omega)_{B_{i}B_{j};B_{3}B_{4}}$$

$$E_{B_{i}}(\vec{k}) = M_{B_{i}} + \frac{\hbar^{2}k^{2}}{2M_{B_{i}}} + \frac{1}{\Omega} \sum_{B_{i}} \sum_{\vec{k}'} n_{B_{j}} (|\vec{k}'|) \langle \vec{k}\vec{k}' | G(\omega)_{B_{i}B_{j};B_{i}B_{j}} | \vec{k}\vec{k}' \rangle_{A}$$



#### ♦ Brueckner-Hatree-Fock EoS

$$\varepsilon_{BHF} = \frac{1}{\Omega} \sum_{B_i} \sum_{\vec{k}} n_i (|\vec{k}|) \left( M_{B_i} + \frac{\hbar^2 k^2}{2M_{B_i}} + \frac{1}{2\Omega} \sum_{B_j} \sum_{\vec{k}'} n_{B_j} (|\vec{k}'|) \left\langle \vec{k} \vec{k}' \middle| G(\omega)_{B_i B_j; B_i B_j} \middle| \vec{k} \vec{k}' \middle\rangle_A \right)$$



✓ Pauli blocking

✓ Baryon dressing

Infinite summation of two-hole line diagrams

### ♦ Pressure & Chemical equilibrium

$$P = \rho^2 \frac{\partial (\varepsilon/\rho)}{\partial \rho}$$
,  $\mu_i = b_i \, \mu_n - q_i \, \mu_e$ ,  $\mu_i = \frac{\partial \varepsilon}{\partial \rho_i}$  with  $\varepsilon = \varepsilon_{BHF} + \varepsilon_{3NF} + \varepsilon_{Lepton}$ 

# Interaction Uncertainties & Their Propagation

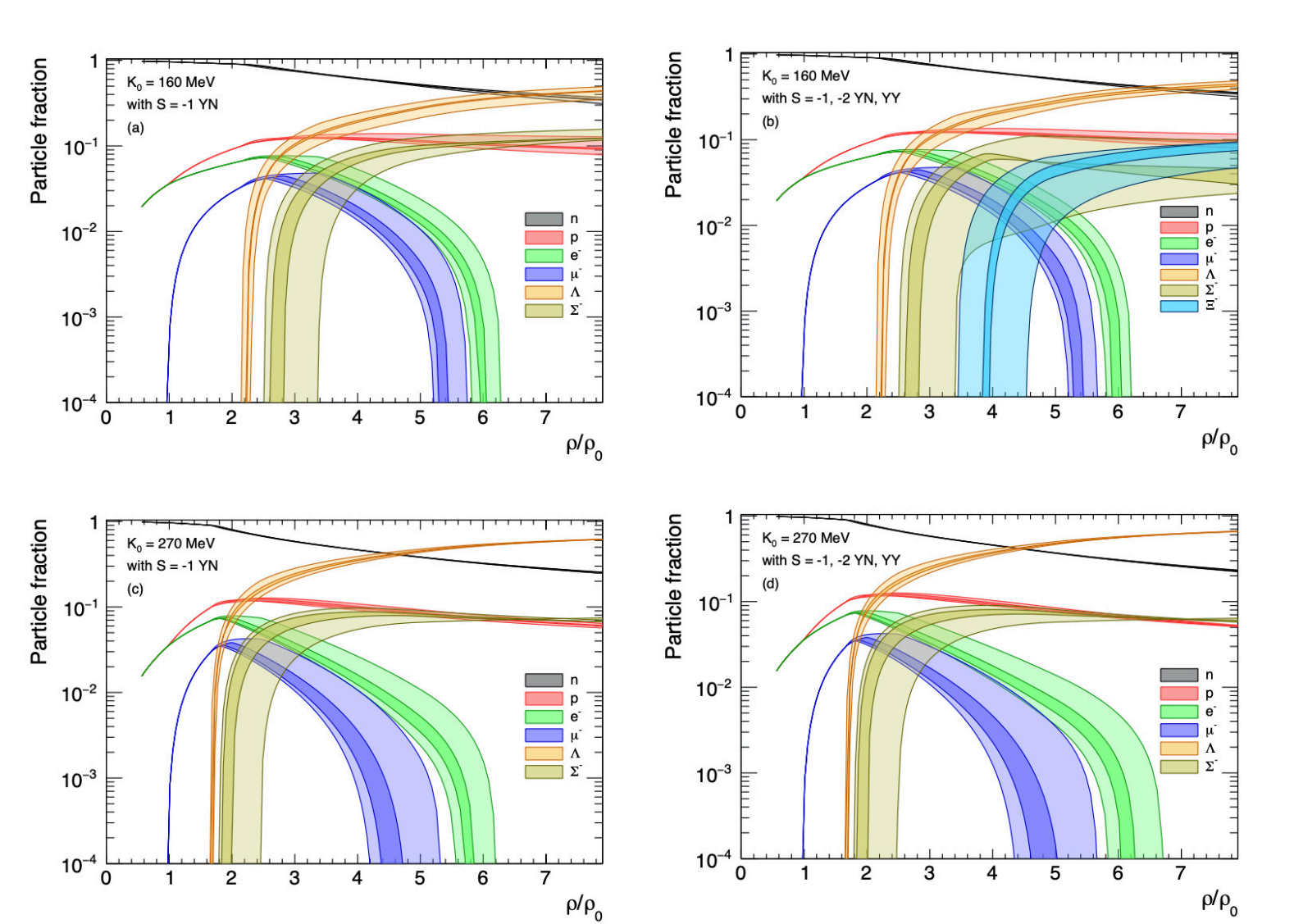
### ♦ Uncertainty sources

- Softness/stiffness of pure nucleonic part explored considering two extreme values of K<sub>0</sub> compatible with current experimental data
- Uncertainty due to the experimental error of femtoscopic  $\Lambda p$  data used to fix the chiral YN interaction & theoretical uncertainty from the residual cut-off dependence of this interaction
- Statistical error of the fitting parameters of the HAL QCD potentials

### ♦ Propagation to the NS properties

- Experimental error of femtoscopic data: For each one of the two pure nucleonic EoS we perform all possible calculations combining the variants I of the NLO19 YN interaction with a cutoff value of 600 MeV and the LECs tuned to  $\Lambda p$  femtoscopic data with HALQCD potentials corresponding to two sets of parameters selected out of the 71 used by the ALICE Collaboration in their analysis of the  $\mathcal{Z}^-p$  CF data corresponding to the less and most attractive  $\Xi N$  interaction.
- Theoretical uncertainty from the residual cut-off dependence: For each one of the two pure nucleonic EoS we perform all possible calculations combining the variants II of the NLO19 YN interactions with cutoff values 500-650 MeV the two sets of the HALQCD potentials just mentioned
- Error bands: defined by those combinations that give the stiffer & softer EoS

# Neutron Star Matter Composition



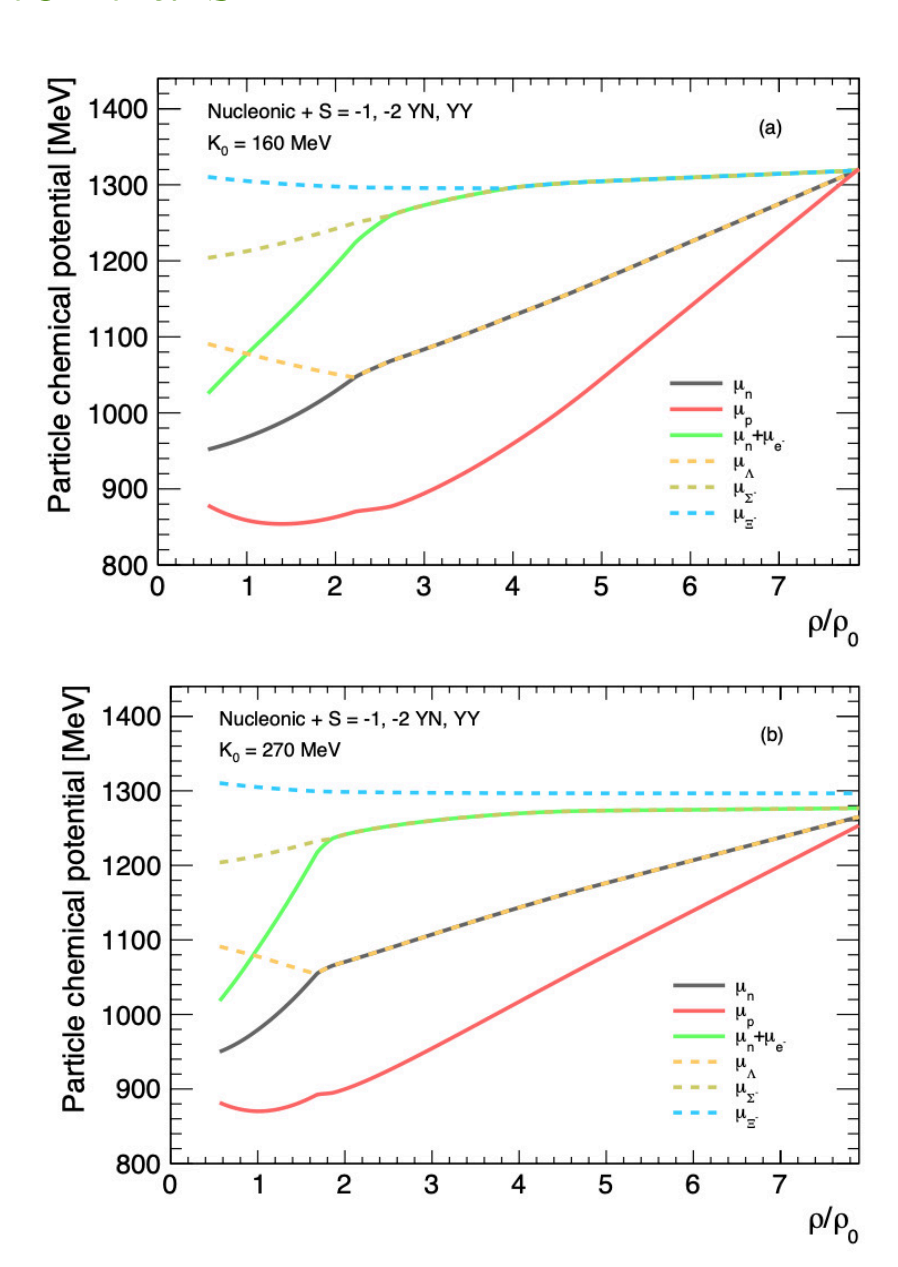
- Onset densities of  $\Lambda$  and  $\Sigma^-$  is the same for the S = -1 & S = -1, -2 case because:
  - $\triangleright$  up to the  $\Lambda$  onset density the S=-2 interactions play no role (matter composed only of nucleons & leptons)
  - $\wedge$  ΛΣ<sup>-</sup> and Σ<sup>-</sup>Σ<sup>-</sup> channels have not been included
- A stiffer pure nucleonic EoS leads to an earlier onset and a slightly larger population of  $\Lambda$  and  $\Sigma^-$
- The  $\Xi^-$  appears around  $4\rho_0$  when a softer nucleonic EoS is considered but it does not appear (or it appears at very large densities) when using a stiffer one.

Narrow bands: uncertainty from femtoscopy. Wider bands: theoretical uncertainty from residual cut-off dependence of NLO19 interactions

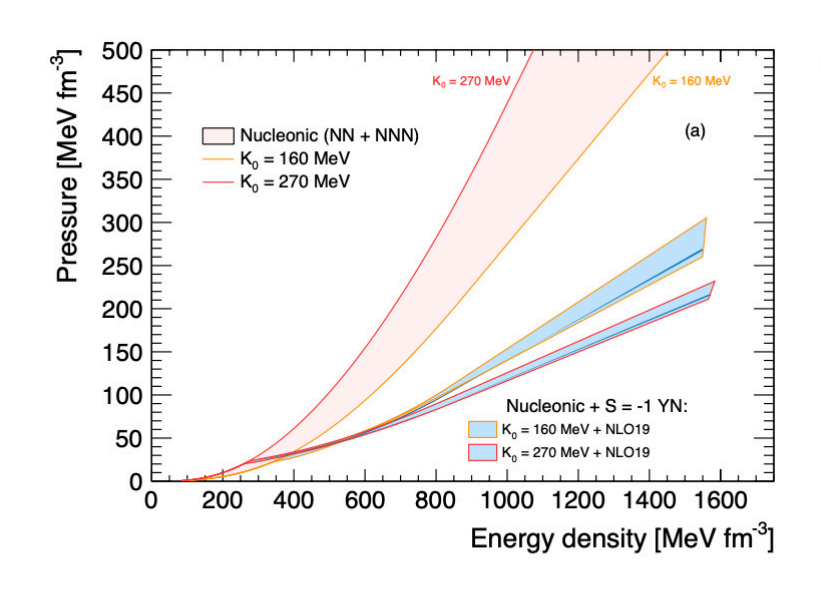
## Particle Chemical Potentials

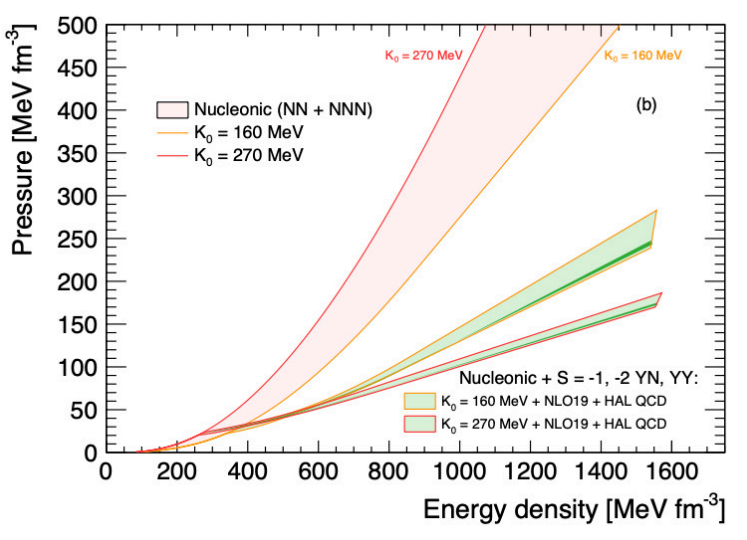
- Earlier onset of  $\Lambda$  and  $\Sigma^-$  when using a stiffer nucleonic EoS (panel b) is due to the fact  $\mu_n$  and  $\mu_n + \mu_e$  increase more rapidly with density ensuring the chemical equilibrium condition for the appearance of both hyperons to be fulfilled at lower densities
- The  $\Xi^-$  which for the softer nucleonic EoS appears at around  $4\rho_0$ , does not appear below  $8\rho_0$  for the stiffer one. The reason is that in this case, due to the earlier appearance of the  $\Sigma^-$ , both neutron and electron chemical potentials are smaller and, therefore, the  $\Xi^-$  onset condition is only fulfilled at very large densities

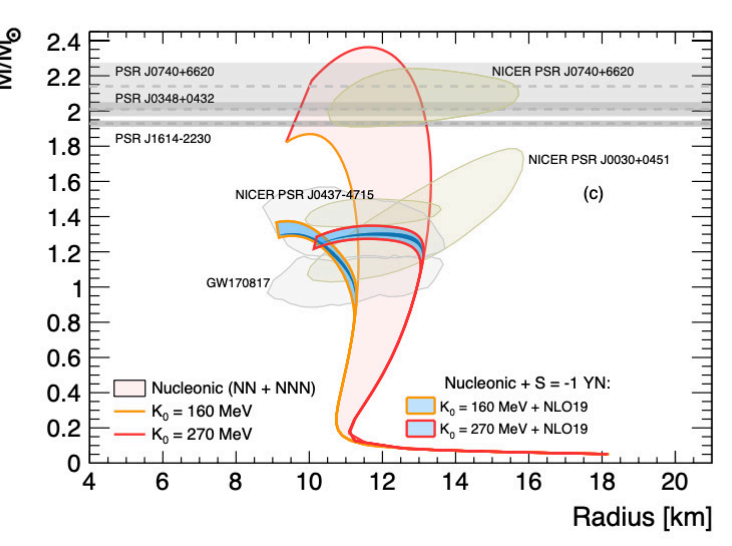
Results shown for the chiral YN potential NLO19 with a cutoff of 600 MeV, and one set of parameters for the  $\Lambda\Lambda$  and  $\Xi N$  HAL QCD potentials

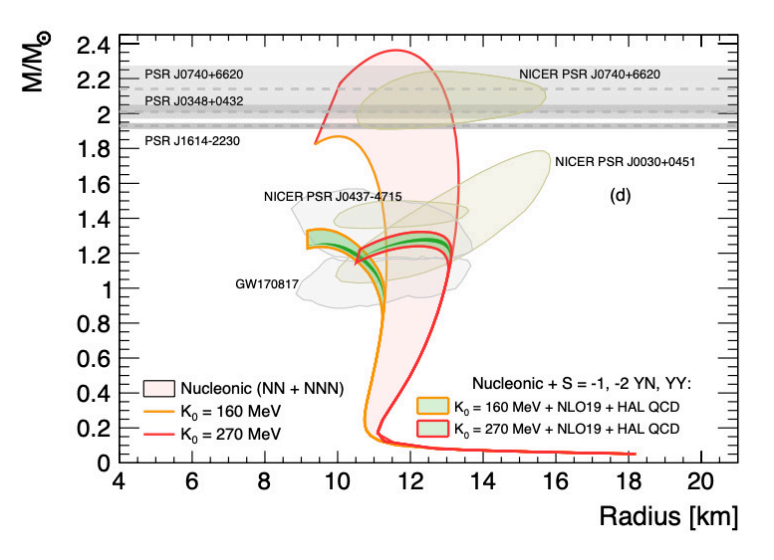


## Neutron Star EoS & Mass-Radius Relation









#### ■ EoS

- As expected hyperons lead to a softening of the FoS
- The softening is enhanced when the nucleonic contribution to the EoS is stiffer because of the earlier appearance of hyperons and their larger population in this case
- Additional softening when taken into account the  $\Lambda\Lambda$  and  $\Xi N$  interactions due to their attractive character

#### Mass-Radius Relation

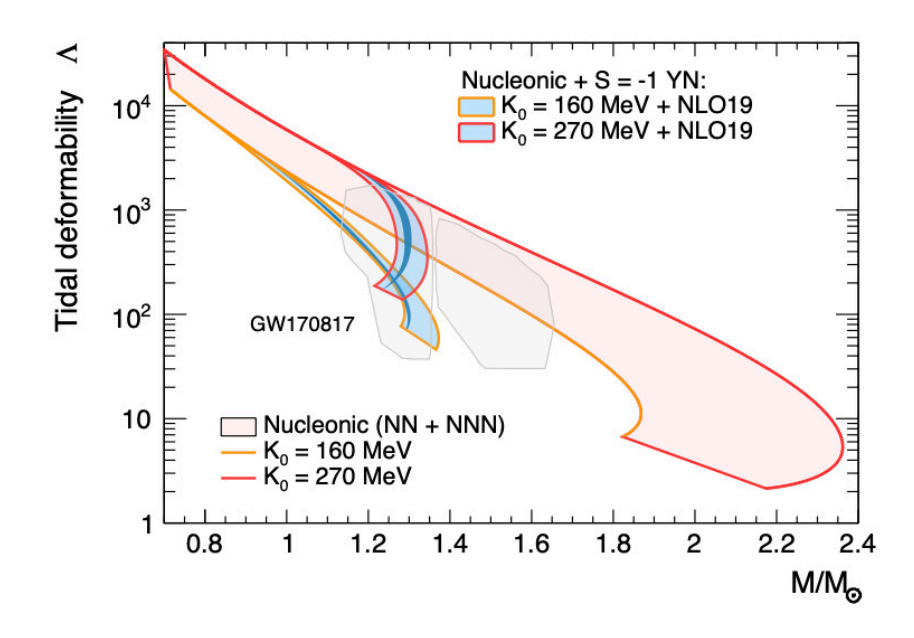
- ightharpoonup M<sub>max</sub> in the range 1.3-1.4 M<sub> $\odot$ </sub>
- ▶  $M_{max}$  quite insensitive to the nucleonic part of the EoS the reason being several compensation mechanism caused by hyperon's appearance that lead always to a soft EoS keeping  $M_{max}$  with about  $0.05~M_{\odot}$

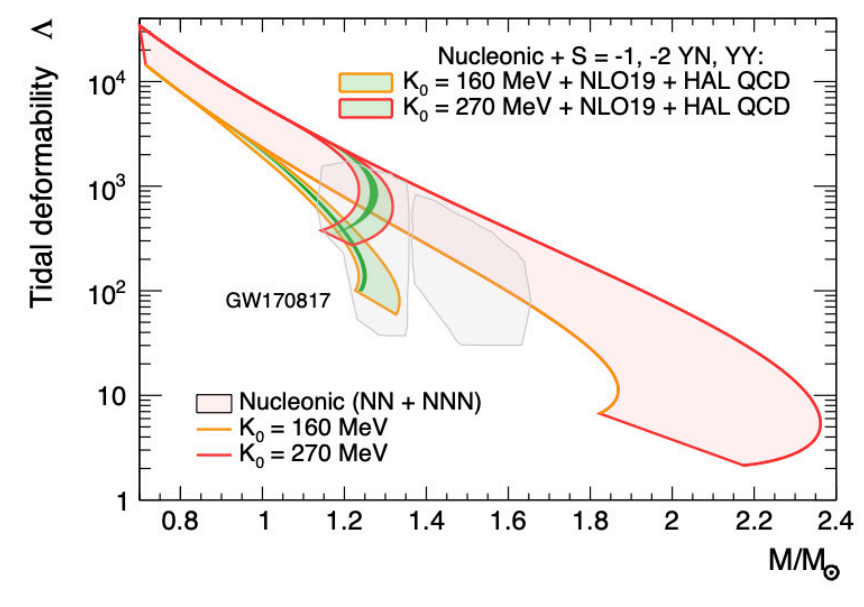
# Tidal Deformability

• At any given value of the stellar mass the tidal deformability of a neutron star with hyperons is always smaller than that of a pure nucleonic because its radius is smaller and, therefore, its compactness C larger

$$\Lambda = \frac{\lambda}{M^5} = \frac{2}{3} \frac{k_2}{C^5}$$
,  $k_2$  tidal Love number,  $C = M/R$ 

■ While the tidal deformability of a pure nucleonic star is fully compatible with the GW170817 constraints, the one predicted for hyperonic stars is only compatible in the range  $1.1\text{-}1.3~\mathrm{M}_{\odot}$ . However, remember that here  $\mathrm{M}_{\mathrm{max}}$  is in the range  $1.3\text{-}1.4~\mathrm{M}_{\odot}$ 





# The final message of this talk



- Construction the hypernuclear matter EoS & study NSs properties using YN & YY interactions compatible with femtoscopic  $\Lambda p$ ,  $\Lambda \Lambda$  and  $\Xi$ -p data from the ALICE Collaboration
- Special attention is put on the uncertainties of the baryon interactions & how they are effectively propagated to the composition, EoS, MR relation & tidal deformability of NSs
  - $\triangleright$  softness/stiffness of pure nucleonic part explored considering two extreme values of  $K_0$  compatible with current experimental data
  - > uncertainty due to the experimental error of femtoscopic Λp data used to fix the chiral YN interaction & theoretical uncertainty from the residual cut-off dependence of this interaction
  - two sets of parameters of the YY HALQCD potentials corresponding to the most and less  $\Xi N$  interaction compatible with femtoscopic data have been used
- Neutron star maximum masses are found to be in the range  $1.3 1.4 \, \mathrm{M}_{\odot}$  in agreement with previous works using microscopic approaches. The hyperon puzzle remains, therefore, an open question if only two-body forces are considered
- Predictions for the tidal deformability are found to be in agreement with the observational constraint from GW170817 in the mass range  $1.1 1.3 \, \mathrm{M}_{\odot}$

- ♦ You for your time & attention
- ♦ My collaborators: Valentina Mantovani
   Sarti, Johann Haidenbauer, Dimitar
   Mihaylov & Laura Fabbietti

